A porosity model to represent the influence of structures on a fluid flow - Application to a hypothetical core disruptive accident

Marie-France Robbe, Fabienne Bliard

7th International Conference on Nuclear Engineering
Tokyo, Japan, April 19-23, 1999
ICONE-7819

A POROSITY MODEL TO REPRESENT THE INFLUENCE OF STRUCTURES ON A FLUID FLOW. APPLICATION TO A HYPOTHETICAL CORE DISRUPTIVE ACCIDENT

Marie-France ROBBE *
DEA, Universite PARIS VI, (Pierre et Marie Curie)
Ecole Centrale de PARIS, Ecole des Mines d'ALES
CEA Saclay - DRN/DMT/SEMT/DYN - 91191 Gif sur Yvette cedex - FRANCE
Tel: (33.1) 69.08.87.49, Fax: (33.1) 69 08 76 19
E-mail: mfr@semt2.smts.cea.fr

Fabienne BLIARD
SOCOTEC Industrie - Service AME - 1 avenue du Parc - 78180 Montigny le Bretonneux - FRANCE
Tel: (33.1) 30.12.85.42, Fax: (33.1) 30.12.85.83
E-mail: bliard@industrie.socotec.fr

Abstract

The internal structures of a Liquid Metal Reactor vessel have a complex geometry. In order to take into account their influence on the fluid flow, without meshing them, during a Hypothetical Core Disruptive Accident, a porosity model was developped and implemented in the CASTEM-PLEXUS code.

The numerical model is described by the mass and momentum modified conservation equations and the HCDA constitutive law. The structure presence is only represented by three parameters: a porosity, a shape coefficient and a pressure loss coefficient.

The new HCDA material is qualified on an analytical shock tube test, representing an horizontal slice of a schematic LMFBR (bubble at high pressure, liquid sodium and internal structures). As we suppose there is no friction, the zone containing structures can be compared to a fluid port reduction. The CASTEM-PLEXUS results are in a good agreement with the theoretical ones.

A short parametric study shows the influence of the porosity and the structure shape on the pressure wave impacting the shock tube bottom. These results will be used to simulate numerically the HCDA mechanical effects in a small scale reactor mock-up.

Keywords: porosity, core disruptive accident, liquid metal reactor, internal structures, qualification

1 Introduction

In case of a Hypothetical Core Disruptive Accident (HCDA) in a Liquid Metal Reactor, the interaction between fuel and liquid sodium creates a high pressure gas bubble in the core. The violent expansion of this bubble loads the vessel and the internal structures, whose deformation is important.

During the 70s and 80s, the LMFBR integrity was studied with codes specially devoted to the analysis of transient loads resulting from a HCDA : SURBOUM, PISCES 2DELK, SEURBNUK/EURDYN, ASTARTE, CASSIOPEE, REXCO, SIRIUS... In order to validate these codes, experimental programmes and benchmarks were undertaken by several countries : COVA, APRICOT, WINCON, MARA, STROVA, CONT...

The SIRIUS french code (Blanchet, 1981) (Daneri, 1981) was validated on the MARA experimental programme (Louvet, 1989) (Bour, 1989). Based on a 1/30 scale model of the SUPER-PHENIX reactor, this programme involves ten tests of gradual complexity due to the addition of internal deformable structures :
• MARA 01/02 consider a vessel partially filled with water and closed by a rigid roof (Acker, 1981),
• MARA 04 represents the main core support structures (Smith, 1985),
• MARA 08/09 are empty and closed by a flexible roof (Fiche, 1985),
• MARA 10 includes the core support structures and a simplified representation of the above core structure (ACS) (Louvet, 1987).
The MARS test rests on a 1/20 scale mock-up including all the significant internal components (Falgayrettes, 1983).

As other codes using a Lagrangian approach, SIRIUS needed rezonings during calculation because the internal structure presence caused high distorsion of the fluid meshes. Finite differences were used for the sodium and the roof and finite elements for the thin vessel. As the argon and the bubble were not meshed, a law related volume to pressure.

At the end of the 80s, it was preferred to add a specific HCDA sodium-bubble-argon tricomponent constitutive law (Lepareux, 1991) to the general ALE fast dynamics finite element CASTEM-PLEXUS code (Hoffmann, 1984). The HCDA constitutive law was qualified (Casadei, 1989) on the CONT benchmark (Benuzzi, 1987).

In order to demonstrate the CASTEM-PLEXUS capability to predict the behaviour of real reactors (Lepareux, 1993) (Cariou, Pirus, 1997), axisymmetrical computations of the MARA serie were confronted with the experimental results. Whereas the CASTEM-PLEXUS results and the MARA 08 and MARA 10 tests (Cariou, 1993) were in a good agreement, the prediction of the MARS structure displacements and strains was overestimated (Cariou, Lepareux, 1997).

This conservatism was mainly due to the fact that several MARS non axisymmetrical structures like core elements, pumps and heat exchangers were not represented in the CASTEM-PLEXUS model. These structures, acting as porous barriers, had a protective effect on the containment by absorbing energy and slowing down the fluid impacting the containment.

For these reasons, we developped in CASTEM-PLEXUS a new HCDA constitutive law taking into account the presence of the internal structures (without meshing them) by means of an equivalent porosity method. The theoretical bases of the method were described by Robbe (1999).

This paper is focused on the description of the sodium-argon-bubble-solid constitutive law implemented in the CASTEM-PLEXUS code, the qualification of the model on a simple test and a short study to assess the influence of the parameters added by the description of the structures.

2 The CASTEM-PLEXUS software

CASTEM-PLEXUS is a french general software, developped by the CEA-Saclay, for 1D, 2D or 3D structure calculations. It is devoted to the analysis of fast transient phenomena. The main fields dealt with are impacts, explosions, pipe circuits and hydrodynamics. Solid and fluid structures can be considered with a possible Fluid-Structure Interaction.

CASTEM-PLEXUS uses the Finite Element Method. The time integration is explicit and the formulation can be Lagrangian, Eulerian or ALE. The code can take into account various non-linearities related to the material or the geometry.

With the library of general elements and constitutive laws, a lot of classical industrial problems can be solved. But to help the nuclear severe accident understanding, some specific constitutive laws were developped for the Liquid Metal Fast Breeder Reactors: a Core Disruptive Accident law and a Sodium-Water Reaction law.

One of the CASTEM-PLEXUS advantages lays on the easiness to introduce new constitutive laws or to modify the existing ones. We used this feature to introduce a solid-porosity model in the existing HCDA constitutive law. This model now allows to analyse the influence of the LMFBR vessel internal structures on the fluid flows inside the vessel during the accident. It also improves the assessment of the mechanical consequences on the vessel.

3 The porous HCDA constitutive law in CASTEM-PLEXUS

3.1 The fluid components

Three fluid components are involved throughout a Hypothetical Core Disruptive Accident in a LMFBR. The initial conditions for a CASTEM-PLEXUS computation of the accident are presented in figure 1.

The vessel is initially filled with liquid sodium topped by an argon cover gas next to the roof. A bubble gas composed of a vaporized fuel mixture is located in the middle of the core.

During the bubble expansion, the sodium can mix with both other components. Because of the probable sodium cavitation, sodium vapour (at saturation conditions) is taken into account.

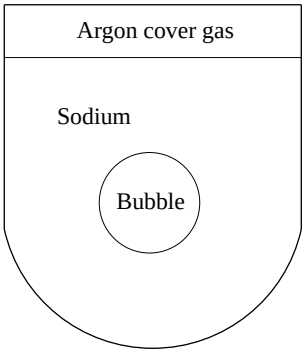

Fig. 1: The initial fluid location in a HCDA

For the purpose of simplificating the numerical model, we consider that the sodium-argon-bubble mixture is homogeneous in each mesh and that the presence of the other components does not infer on the constitutive law of each one. We also assume that there is no thermal transfers between the components during the explosion.

In the finite element model, the nodal variables are the same for all the components. The elementary variables depend on several parameters : the partial variables of each component, the component presence fractions...

3.2 The solid components

The figure 2 represents the internal structures of a LMFBR. The porosity model was specially developped to represent the solid structures of the core (9), the pumps and the heat exchangers (10) which are far too complex to mesh. The other structures are modelled by means of shells.

In the porosity model, the structures are simply described, in an Eulerian formulation, by a porosity $\beta = \Omega_f/\Omega$, a shape coefficient A_S/Ω and an isotropic pressure loss coefficient ξ (Robbe, 1999).

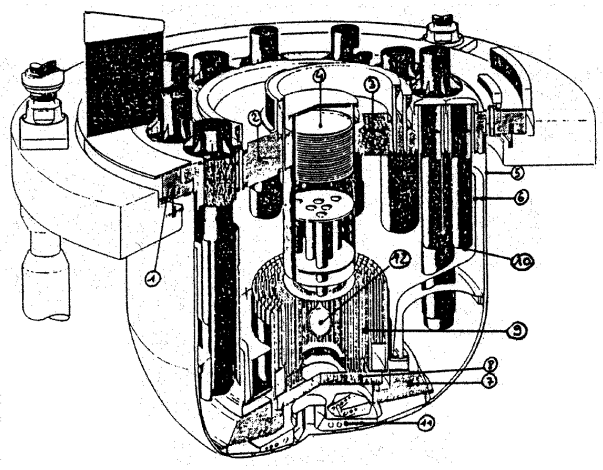

Fig. 2: The internal structures of a LMFBR

3.3 The equations

CASTEM-PLEXUS solves successively, at each time step, the mass conservation law, the constitutive law and then the momentum conservation law. The mass conservation is obtained by balancing the inward and outward fluxes crossing the mesh boundary.

$$\Delta\mathcal{M}^{(n\to n+1)} = -\int_{t^{(n)}}^{t^{(n+1)}} \oint_A \left(\beta\rho_f^{(n)}\right)\vec{v}_f^{(n+1/2)}.\vec{n}\,dA\,dt \quad \text{with} \quad \rho_f = x_a\rho_a + x_b\rho_b + x_s\rho_s + x_v\rho_v$$

Apart from the solid structures which are supposed inert and motionless, the fluid mixture is described by the constitutive laws of each component (Lepareux, 1993):

Argon	:	Perfect gas with an adiabatic behaviour
Bubble	:	Perfect gas described by a polytropic law
Liquid sodium	:	Perfect fluid whose temperature is assumed constant
Sodium vapour	:	The diphasic sodium is at saturation conditions. It only depends on the initial temperature $T^{(0)}$.

$$p_a^{(n+1)} = p_a^{(n)}\left(\frac{\rho_a^{(n+1)}}{\rho_a^{(n)}}\right)^{\gamma_a} \qquad p_b^{(n+1)} = p_b^{(n)}\left(\frac{\rho_b^{(n+1)}}{\rho_b^{(n)}}\right)^{\nu_b} \qquad p_v^{(n+1)} = p_{saturation}\left(T^{(0)}\right)$$

$$p_s^{(n+1)} = p_s^{(n)} + c_s^2\left(\rho_s^{(n+1)} - \rho_s^{(n)}\right) \qquad p_g^{(n+1)} = p_a^{(n+1)} + p_b^{(n+1)} + p_v^{(n+1)}$$

For a mesh containing all the constituents, the final pressure is $p_f^{(n+1)} = p_s^{(n+1)} = p_g^{(n+1)}$. The pressure is obtained by iteration.

The density and the pressure of the homogeneous fluid are then used to calculate the fluid acceleration from the momentum conservation. The variational formulation of the momentum equation can be written:

$$\underbrace{\int_\Omega \vec{\mathcal{U}}^*.(\beta\,\rho_f)\frac{\partial \vec{v}_f}{\partial t}\,d\Omega}_{\mathcal{M}^{(n+1)}\,\vec{\gamma}^{(n+1)}} + \underbrace{\int_\Omega \vec{\mathcal{U}}^*.\left[(\beta\,\rho_f)\,\vec{v}_f.\overline{\overline{\dot{\epsilon}}}_f\right]d\Omega}_{\text{transport force}} - \underbrace{\oint_A \left[\vec{\mathcal{U}}^*.(\beta\,\overline{\overline{\sigma}}_f)\right].\vec{n}\,dA}_{\text{boundary conditions}} + \underbrace{\int_\Omega \overline{\overline{\epsilon}}^* : (\beta\,\overline{\overline{\sigma}}_f)\,d\Omega}_{\text{internal force}}$$

$$- \underbrace{\int_\Omega \vec{\mathcal{U}}^*.p_f\left(\vec{\nabla}\beta\right)d\Omega}_{\text{force between 2 porous media}} + \underbrace{\int_\Omega \vec{\mathcal{U}}^*.\left[\frac{1}{2}\frac{A_S}{\Omega}\,\xi\,(\beta\,\rho_f)\,|\vec{v}_f|\,\vec{v}_f\right]d\Omega}_{\text{fluid-solid interaction force}} = \vec{0}$$

$$\text{with} \qquad \beta\,\overline{\overline{\sigma}}_f = -\beta\,p_f\,\overline{\overline{I}} - \frac{2}{3}\,(\beta\,\mu_f)\left(\text{tr}\,\overline{\overline{\dot{\epsilon}}}_f\right)\overline{\overline{I}} + 2\,(\beta\,\mu_f)\,\overline{\overline{\dot{\epsilon}}}_f$$

The final velocity $\vec{v}^{(n+1)}$ is easily deduced from the acceleration $\vec{\gamma}^{(n+1)}$.

4 Qualification of the numerical model on a shock tube test

Before the porous model is applied to a reactor computation to predict the mechanical consequences of a HCDA, it is necessary to qualify the model on an analytical test. We chose to study a HCDA in a shock tube (fig. 3) representing a half-reactor horizontal slice and to compare the CASTEM-PLEXUS results with theoretical ones. Both shock tube extremities are bounded by absorbing conditions, prohibiting thus the wave reflections on the bottoms.

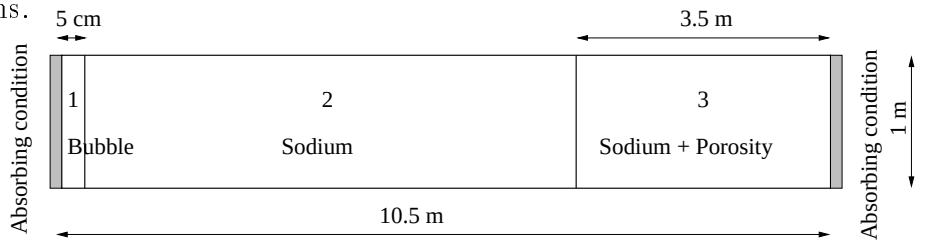

Fig.3: Shock tube representing a HCDA

The shock tube is 10.5 m long which corresponds to a reactor radius. It is 1 m high and 1 m wide, so its section is 1 m^2. The first material on the left is a bubble at 10 MPa; it represents the bubble created by the vaporized fuel mixture in the middle of the core, on the reactor axisymmetrical axis. The rest of the shock tube contains sodium at the reactor nominal pressure (0.3 MPa).

The third material on the right is a mixture of sodium and solid structures; it represents the pump and heat exchanger zone characterized by a porosity $\beta = 0.5$. We suppose there is no fluid-solid friction, so the solid presence is only described by the porosity. In a 1D case, the mass equation simplifies in such a way that the problem can come down to a shock tube presenting a section change (fig. 4). The tube narrow part is such as the fluid port is half the tube section: $\beta\,S_3 = 0.5$ m^2.

Fig.4: Equivalent shock tube with a section change

The characteristics of each shock tube zone are defined as follows:

Bubble	Sodium	Sodium + Solid
$S_1 = 1$ m^2	$S_2 = 1$ m^2	$S_3 = 0.5$ m^2
$\rho_1 = 2430$ kg/m^3	$\rho_2 = 856$ kg/m^3	$\rho_3 = 856$ kg/m^3
$p_1 = 10$ MPa	$p_2 = 0.3$ MPa	$p_3 = 0.3$ MPa
$c_1 = \sqrt{\gamma_1 \, p_1/\rho_1} = 73.14$ m/s	$c_2 = 2368$ m/s	$c_3 = 2368$ m/s
$\gamma_1 = 1.3$	$p_{2_{saturation}} = 53.2$ MPa	$p_{3_{saturation}} = 53.2$ MPa
$\nu_1 = 0.545$	$\rho_{2_{vapour}} = 0.001$ kg/m^3	$\rho_{3_{vapour}} = 0.001$ kg/m^3

Let us compare the porosity model results with the theoretical results of a section change. Let us set in the acoustical hypothesis. At the interface level between zone 2 and zone 3, the incident wave splits up into a reflected wave propagating in the opposite direction and in the same medium, and into a transmitted wave propagating in the same direction but in the medium on the other side of the interface.

The pressure variations and the flow rates are the same on both interface sides (Royer, 1996), thus: $\delta p_2 = \delta p_3$ and $q_2 = q_3$. These conditions can be written:

$$\delta p_{i_2} + \delta p_{r_2} = \delta p_{t_3} \qquad \text{and} \qquad S_2 \, (\delta v_{i_2} + \delta v_{r_2}) = S_3 \, \delta v_{t_3}$$

As the overpressure is defined by $\delta p = \pm \, \rho \, c \, \delta v$ according to the wave direction, we then must solve:

$$\begin{cases} \rho_2 \, c_2 \, (\delta v_{i_2} - \delta v_{r_2}) = \rho_3 \, c_3 \, \delta v_{t_3} \\ S_2 \, (\delta v_{i_2} + \delta v_{r_2}) = S_3 \, \delta v_{t_3} \end{cases}$$

As a result, the pressures and velocities are:

$$\delta p_{i_2} = 9.7 \text{ MPa} \qquad \delta v_{i_2} = \frac{\delta p_{i_2}}{\rho_2 \, c_2} = 4.7854 \text{ m/s}$$

$$\delta v_{r_2} = \frac{S_3 - S_2}{S_2 + S_3} \, \delta v_{i_2} = -1.5951 \text{ m/s} \qquad \delta v_{t_3} = \frac{2 \, S_2}{S_2 + S_3} \, \delta v_{i_2} = 6.3805 \text{ m/s}$$

$$\delta p_{r_2} = \frac{S_2 - S_3}{S_2 + S_3} \, \delta p_{i_2} = 3.233 \text{ MPa} \qquad \delta p_{t_3} = \frac{2 \, S_2}{S_2 + S_3} \, \delta p_{i_2} = 12.933 \text{ MPa}$$

$$p_{2_{interface}} = p_2^{(0)} + \delta p_{i_2} + \delta p_{r_2} = 13.233 \text{ MPa} \qquad p_3 = p_3^{(0)} + \delta p_{t_3} = 13.233 \text{ MPa}$$

$$v_{2_{interface}} = v_2^{(0)} + \delta v_{i_2} + \delta v_{r_2} = 3.1903 \text{ m/s}$$

Let us compare the theoretical results with the CASTEM-PLEXUS ones.

Location	Time (ms)	p_{theory} (MPa)	$p_{calculation}$ (MPa)	$\Delta p/p$ (%)	δv_{theory} (m/s)	$\delta v_{calculation}$ (m/s)	$\Delta(\delta v)/\delta v$ (%)
1: left	0	10	10	0	–	–	–
2: left	0.02	10	9.7	3	–	–	–
2: middle	1.47	10	9.6	4	4.79	4.79	0
2: right	2.96	13.2	12.7	3.8	3.19	3.02	5.3
3: left	2.96	13.2	13.2	0	3.19	3.02	5.3
3: right	4.43	13.2	12.3	6.8	6.38	6.02	5.6

The results are presented on the figures 5 and 6. The CASTEM-PLEXUS results are in good agreement with the theoretical results. The small discrepancies, especially observed in the third zone, are caused by the discrete finite element meshing and a slight numerical diffusion.

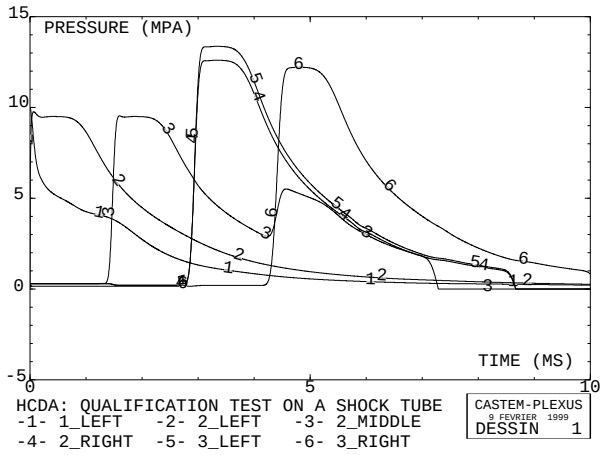

Fig. 5: Pressures

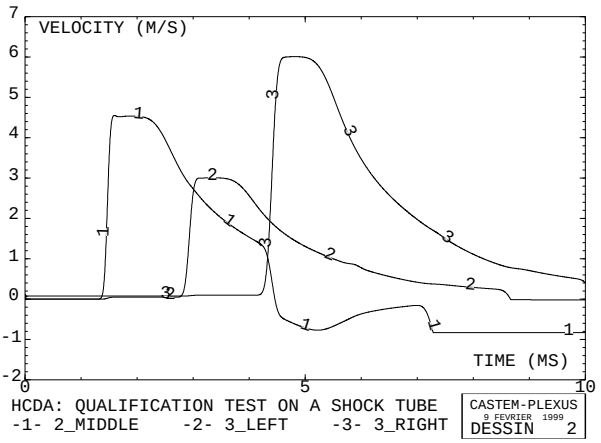

Fig. 6: Fluid velocities

5 Influence of the parameters representing the structures

In order to assess the influence of the parameters describing the structures on the global fluid flow, we carried out a short parametric study on the previous shock tube geometry. We focused on the solid density and the structure shape.

We considered three solid densities. The parameter $\beta = 1$ describes a fluid without structures. The porosity $\beta = 0.8$ corresponds to a medium containing a few structures. The value $\beta = 0.5$ represents a fluid cluttered with a great quantity of structures. Beyond $\beta = 0.2$, the problem is closer to a fluid dropping through a porous solid net and the model developped in CASTEM-PLEXUS may not suit the physical problem.

For both $\beta = 0.8$ and $\beta = 0.5$ porosity coefficients, we studied a case without fluid-solid friction and two kinds of structure shape: a single big obstacle and a set of small scattered structures. We chose an horizontal cylinder (fig. 7) and a vertical tube bundle (fig. 8).

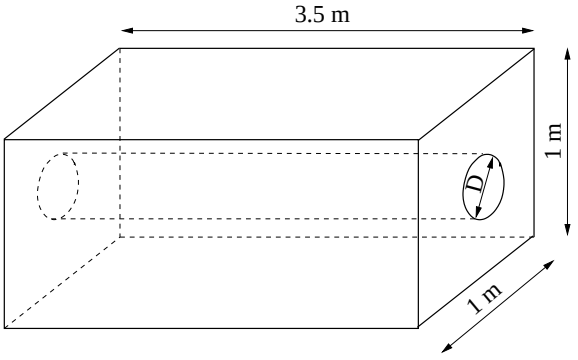

Fig. 7: A single cylinder

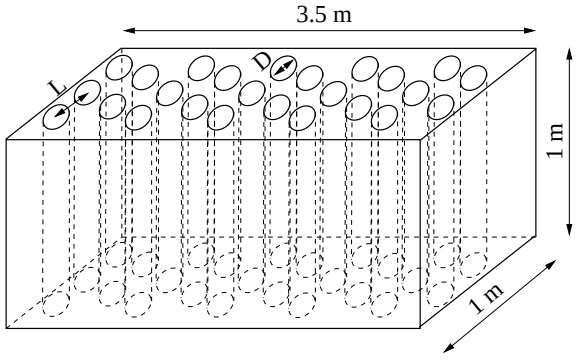

Fig. 8: A tube bundle

The solid parameters and the CASTEM-PLEXUS results are summerized in the following table. The pressure loss coefficient ξ is given by Idel'Cik (1986) on page 367 for the single cylinder and page 314 for the staggered tube bundle. The pressures are in MPa and the velocities in m/s.

$\beta = 1$	$\beta = 0.8$	$\beta = 0.8$	$\beta = 0.8$	$\beta = 0.5$	$\beta = 0.5$	$\beta = 0.5$
no friction	no friction	cylinder	bundle	no friction	cylinder	bundle
			3 trans. rows 14 leng. rows 35 tubes L = 0.25 m			5 trans. rows 20 leng. rows 90 tubes L = 0.167 m
		D = 0.5 m	D = 0.16 m		D = 0.8 m	D = 0.158 m
$\frac{A_S}{\Omega} = 0$	$\frac{A_S}{\Omega} = 0$	$\frac{A_S}{\Omega} = 1.585$	$\frac{A_S}{\Omega} = 5.01$	$\frac{A_S}{\Omega} = 0$	$\frac{A_S}{\Omega} = 2.51$	$\frac{A_S}{\Omega} = 12.71$
		$c_x = 0.99$ $\tau = 1.5$ $\xi_h = 0.72$	$\mathcal{A} = 3.2$ $Re = 4250$		$c_x = 0.88$ $\tau = 1.5$ $\xi_h = 36.61$	$\mathcal{A} = 7.23$ $Re = 4250$
$\xi = 0$	$\xi = 0$	$\widehat{\xi} = 0.52$	$\xi = 1.696$	$\xi = 0$	$\widehat{\xi} = 26.20$	$\xi = 4.60$
$p_f = 9.4$	$p_f = 10.4$	$p_f = 10.3$	$p_f = 10.2$	$p_f = 12.3$	$p_f = 10.5$	$p_f = 10.8$
$\beta p_f = 9.4$	$\beta p_f = 8.32$	$\beta p_f = 8.24$	$\beta p_f = 8.16$	$\beta p_f = 6.15$	$\beta p_f = 5.25$	$\beta p_f = 5.40$
$v_f = 4.6$	$v_f = 5.15$	$v_f = 5.1$	$v_f = 5.0$	$v_f = 6.02$	$v_f = 5.2$	$v_f = 5.3$

The fluid pressure and the fluid velocity are read on the right side of zone 3. As the bottom shock tube simulates the reactor vessel, we are interested in estimating the effect of the structure taking into account on the force impacting the vessel.

Because of the port reduction for the fluid, the structure presence leads to a local increase of the fluid pressure p_f and the fluid velocity v_f. The fluid velocity is not zero on the shock tube bottom because the absorbing condition makes believe to an infinite tube.

The impact force is composed of an internal force (pressure term) and a transport force (term of spatial derivative of the kinetic energy). The boundary condition term introduces no force for an absorbent.

The results show that the average pressure βp_f received by the shock tube bottom decreases when the structure density increases. The average transport force decreases too because it is weighted by β. Thus, the impact force lowers with the structure presence. As planned, we check that the structures act as a protection shield for the shock tube bottom.

The fluid-solid interaction force, represented by the parameters A_S/Ω and ξ, slightly slows down the fluid and makes the average pressure decrease a little more. This force is very similar to a loss of kinetic energy. We obtain more or less the same results with the cylinder and the tube bundle because the product $\frac{A_S}{\Omega}\xi$ is practically the same for both solid distributions.

The most influential parameter is the porosity. The average pressure is 35 % lower with $\beta = 0.5$ than without structures. The fluid-solid interaction force adds a pressure reduction ranging from 1 to 10 %.

6 Conclusion

This paper briefly describes the porosity model implemented in the CASTEM-PLEXUS code to represent the structure presence into a fluid flow. The numerical qualification of the model on a shock tube test shows that the CASTEM-PLEXUS results are in a good agreement with the theoretical ones. The parametric study proves that the internal structures have a shield effect against the fluid wave impacting the LMFBR vessel in case of a HCDA.

The porosity method will be used for representing some internal structures (pumps and heat exchangers) of the MARS mock-up, simulating a HCDA in a small scale reactor. That should improve the results of the numerical simulation. More generally, this method can be adapted to any kind of problem involving a fluid flow getting through a structure set of complex shape.

7 Nomenclature

Superscripts

(n)	time step

Subscripts

a	argon	b	bubble gas
f	fluid	g	gas
i	incident wave	r	reflected wave
s	liquid sodium	S	solid
t	transmitted wave	v	sodium vapour
$1, 2, 3$	shock tube zones		

Variables

A	mesh bounding surface	A_S	solid bounding surface
$\mathcal{A}, c_x, \tau$	pressure loss function parameters	c	sound velocity
D	tube diameter	$\overline{\overline{I}}$	unit tensor
L	length between 2 tube centres	$\mathcal{M}$	mass
$\vec{n}$	unit vector normal to a surface	p	pressure
δp	pressure variation	q	flow rate
Re	Reynolds number	S	shock tube section
t	time	$\vec{\mathcal{U}}^*$	arbitrary displacement
$\vec{v}$	velocity	$\lvert\vec{v}\rvert$	norm of the velocity
δv	unidirectional velocity variation	x	volumic presence fraction
β	porosity	$\vec{\nabla}\beta$	gradient of β
$\overline{\overline{\epsilon}}$	spatial derivative of the strain	tr $\overline{\overline{\epsilon}}$	sum of the diagonal terms of $\overline{\overline{\epsilon}}$
$\overline{\overline{\epsilon^*}}$	spatial derivative of $\vec{\mathcal{U}}^*$	γ	heat capacities ratio
$\vec{\gamma}$	acceleration	μ	dynamic or turbulent viscosity
ν	polytopic coefficient (any positive value,ν=1 isothermal law,$\nu=\gamma$ adiabatic law)		
Ω	mesh volume	ρ	density
$\overline{\overline{\sigma}}$	total stress	ξ	isotropic pressure loss coefficient
ξ_h	ξ halfway up the shock tube	$\widehat{\xi}$	ξ averaged on the shock tube height

8 References

Acker, D., Benuzzi, A., Yerkess, A., Louvet, J.: "MARA 01/02 - Experimental validation of the SEURBNUK and SIRIUS containment codes", Proc. Smirt 6, Vol. E 3/6, (1981).

Benuzzi, A.: "Comparison of different LMFBR primary containment codes applied to a benchmark problem", J. Nuclear Engineering Design, Vol. 100, pp 239-249, (1987).

Blanchet, Y., Obry, P., Louvet,J.: "Treatment of fluid-structure interaction with the SIRIUS computer code", Proc. Smirt 6, Vol. B 8/8, (1981).

Bour, C., Sperandio, M., Louvet, J., Rieg, C.: "LMFBR's core disruptive accident. Mechanical study of the reactor block", Proc. Smirt 10, Vol. E, pp 281-287, (1989).

Cariou, Y., Lepareux, M., Noe, H.: "LMR's whole core accident. Validation of the PLEXUS code by comparison with MARS test", Proc. Smirt 14, Vol. P 2/6, (1997).

Cariou, Y., Pirus, J.P., Avallet, C.: "LMR large accident analysis method", Proc. Smirt 14, Vol. P 3/7, (1997).

Cariou, Y., Sperandio, M., Lepareux, M., Christodoulou, K.: "LMFBR's whole core accident. Validation of the PLEXUS code by comparison with MARA tests", Proc. Smirt 12, Vol. E 7/4, (1993).

Casadei, F., Daneri, A., Toselli, G.; "Use of PLEXUS as a LMFBR primary containment code for the CONT benchmark problem", Proc. Smirt 10, Vol. E 13/1, (1989).

Daneri, A., Toselli, G., Trombetti, T., et al.: "Influence of the representation models of the stress-strain law on the LMFBR structures in an HCDA", Proc. Smirt 6, Vol. E 4/4, (1981).

Falgayrettes, M., Fiche, C., Granet, P., et al.: "Response of a 1/20 scale mock up of the Superphenix breeder reactor to an HCDA loading simulation", Proc. Smirt 7, Vol. E 4/1, (1983).

Fiche, C., Louvet, J., Smith, B.L., Zucchini, A.: "Theoretical experimental study of flexible roof effects in an HCDA's simulation", Proc. Smirt 8, Vol. E 4/5, (1985).

Hoffmann, A., Lepareux, M., Schwab, B., Bung, H.: "Plexus - A general computer program for fast dynamic analysis", Proc. Conf. on Structural Analysis and Design on Nuclear Power Plant, Porto Alegre, Bresil, (1984).

Idel'cik, I.E.: "Memento des pertes de charge. Coefficients de pertes de charge singulieres et de pertes de charge par frottement", Collection de la DER d'EDF, Eyrolles, Paris, (1986).

Lepareux, M., Bung, H., Combescure, A., Aguilar, J.: "Analysis of a CDA in a LMFBR with a multiphasic and multicomponent behaviour law", Proc. Smirt 11, Vol. E 13/1, (1991).

Lepareux, M., Bung, H., Combescure, A., et al.: "Analysis of an HCDA in a fast reastor with a multiphase and multicomponent behavior law", Proc. Smirt 12, Vol. E 7/2, (1993).

Louvet, J.: "Containment response to a core energy release. Main experimental and theorical issues. Future trends", Proc. Smirt 10, Vol E, pp 305-310, (1989).

Louvet, J., Hamon, P., Smith, B.L., Zucchini, A.: "MARA 10: an integral model experiment in support of LMFBR containment analysis", Proc. Smirt 9, Vol. E, (1987).

Robbe, M.F.: "A porosity method to model the internal structures of a reactor vessel", Proc. Smirt 15, Vol. B. (1999).

Royer, D., Dieulesaint, E.: "Ondes elastiques dans les solides. Tome 1. Propagation libre et guidee", Enseignement de la physique, Masson, Paris, pp 8-40, (1996).

Smith, B.L., Fiche, C., Louvet, J., Zucchini, A.: "A code comparison exercise based on the LMFBR containment experiment MARA-04", Proc. Smirt 8, Vol. E 4/7, (1985).